2013 American Control Conference (ACC)
Washington, DC, USA, June 17-19, 2013

Enhancing Performance through Multivariable Weighting Function Design in $\mathscr{H}_\infty$ Loop-Shaping: With Application to a Motion System

Frank Boeren, Robbert van Herpen, Tom Oomen, Marc van de Wal, Okko Bosgra

Abstract— **The quality of model-based controllers hinges on a careful specification of performance and robustness requirements. In typical norm-based control designs, these performance and robustness requirements are specified in a scalar optimization criterion, even for complex multivariable systems. This paper aims to develop a novel and systematic approach for the formulation of this optimization criterion for complex multivariable systems. Hereto, characteristics of the underlying system are exploited. In contrast to pre-existing approaches that typically lead to multiloop SISO weighting functions, the proposed approach enables the design of multivariable weighting functions. Experimental results confirm that the proposed procedure significantly improves the performance of an industrial motion system compared to earlier approaches.**

I. INTRODUCTION

The design of a high-performance controller for a complex multivariable system hinges on the specification of a suitable optimization criterion. In model-based control, a scalar criterion is typically adopted that should reflect the user-defined performance and robustness requirements [1], [2], [3]. These requirements are defined in the optimization criterion by means of weighting functions. Since any stabilizing controller is $\mathscr{H}_\infty$-optimal for a certain choice of weighting functions [4], it is essential for the resulting controller that the weighting functions accurately represent the performance and robustness requirements. Indeed, applications of model-based control, see, e.g., [5] for motion systems and [6] for aircrafts, focus on the design of weighting functions.

The $\mathscr{H}_\infty$-optimization methodology is a powerful tool for control design of complex multivariable systems, since it explicitly takes robustness into account. However, most reported design approaches and applications are aimed at single-input, single-output (SISO) systems, see, e.g., [2], [7] and [8]. The first steps to apply $\mathscr{H}_\infty$-control to multivariable systems is restricted to the class of systems that can be approximated as multiloop SISO systems, see, e.g., [9] and [5]. However, this assumption constrains the attainable performance of a complex multivariable system. Therefore, for the general class of multivariable systems, a different path is pursued in, e.g., [10] and [11]. However, this design approach requires fitting of real rational transfer functions to magnitude data. Inaccuracies that typically occur in fitting introduce conservatism in the specification of closed-loop requirements in the optimization criterion. To avoid the problems associated with fitting, in [12] a systematic procedure is proposed that circumvents these problems. However, this procedure is focussed on SISO systems, and provides no straightforward generalization to multivariable systems.

Although $\mathscr{H}_\infty$ control is promising for the design of controllers for complex multivariable systems, at present there exists no systematic procedure for the formulation of performance and robustness requirements for such systems in a scalar optimization criterion. This paper aims to improve the control goal formulation for a class of motion systems.

The main contribution of this paper is a systematic procedure for multivariable weighting function design in the $\mathscr{H}_\infty$ control framework for motion systems with pronounced multivariable dynamical behavior. Hereto, properties of a specific class of mechanical systems are explored to explicitly incorporate the directionality that is associated with lightly damped resonance phenomena in the weighting functions. This enables the specification of performance goals in the control goal formulation for dynamical behavior up to higher frequencies compared to [5], resulting in improved closed-loop performance for motion systems with pronounced multivariable behavior. This performance improvement is illustrated by means of an experimental confrontation with an industrial high-performance motion system.

Remark: In order to clearly illustrate the concepts in this paper, attention is restricted to square systems P. Extensions to non-square systems are conceptually straightforward. The concepts in this paper are presented in continuous time, but are also applicable to sampled-data systems [13].

II. PROBLEM FORMULATION

A. Loop-shaping

In loop-shaping, the goal is to attain a target loop-shape $P_{s,des}$ that prescribes the desired gains of the system as a function of frequency. This target loop-shape reflects closed-loop performance and robustness requirements that are specified by the designer. To attain this loop-shape, the given system P is appended with weighting functions.

Definition 1. *Let $P \in \mathscr{R}^{n\times n}$ be a given system, and $W_1, W_2 \in \mathscr{R}^{n\times n}$ be weighting functions. The shaped system P_s is defined*

$$P_s = W_2 P W_1,$$

where it is assumed that W_1 and W_2 are such that P_s contains no hidden unstable modes.

Remark 2. *The open-loop weighting functions W_1, W_2 can be translated in equivalent closed-loop weighting functions, as advocated in, e.g., [3] and [5]. Equivalence holds if W_1, W_2 satisfy the stringent requirements posed in [2, Section 4.5].*

Frank Boeren, Robbert van Herpen, Tom Oomen and Okko Bosgra are with the Eindhoven University of Technology, The Netherlands (corresponding author: f.a.j.boeren@tue.nl)

Marc van de Wal is with ASML Research, Veldhoven, The Netherlands.

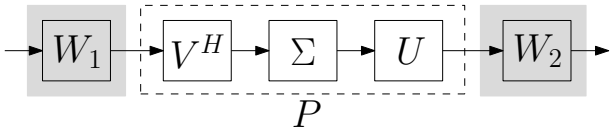

Fig. 1. A need for directionality compensation in weighting functions.

Goal 3. *Given $\sigma_i(P_{s,\text{des}})$, the goal in loop-shaping is to design W_1, W_2 such that*

$$\sigma_i(P_s) \approx \sigma_i(P_{s,\text{des}}) \quad i = 1, \ldots, n.$$

Note that for SISO systems, the role of W_1 and W_2 is interchangeable, i.e., $P_s = WP$ with $W = W_1 W_2$. Indeed, by selecting an appropriate scalar W, the gain of P_s can be straightforwardly manipulated since $\sigma(P_s) = \sigma(W)\sigma(P)$. This observation is exploited in [2], [7] and [8].

For multivariable systems, the construction of W_1 and W_2 to attain $P_{s,des}$ is more involved, due to input and output directionality. This directionality determines the connection between the singular values and the individual entries of P, as reflected in the singular value decomposition.

Definition 4. *Let $P \in \mathscr{R}^{n\times n}$, where $\mathscr{R}$ is the set of real-rational transfer function matrices. Define the singular value decomposition at frequency ω_k as:*

$$P(j\omega_k) = U(j\omega_k)\Sigma(j\omega_k)V^H(j\omega_k), \tag{1}$$

with $\Sigma(j\omega_k) = \text{diag}(\sigma_1(j\omega_k), \sigma_2(j\omega_k), \ldots, \sigma_n(j\omega_k)) \in \mathbb{R}^{n\times n}$ and unitary matrices $V(j\omega_k) \in \mathbb{C}^{n\times n}$ and $U(j\omega_k) \in \mathbb{C}^{n\times n}$.

In (1), Σ represents the gains of the system, while V and U represent the corresponding input and output directionality. Therefore, loop-shaping of the gains of the system requires that W_1 and W_2 explicitly account for the directionality of the system, as illustrated in Fig. 1. For the general class of multivariable systems, this would require full weighting matrices W_1, W_2, which are difficult to design.

B. Classical performance and robustness requirements

Classical loop-shaping design for multivariable systems typically aims at specifying low- and high-frequent asymptotes in $P_{s,\text{des}}$. In particular, the following two requirements are often pursued, see, e.g., [2, Chap. 6] and [3, Chap. 9], which are indicated by the black triangles in Fig. 2.

Definition 5. *The target loop-shape $P_{s,\text{des}}$ is characterized by the following two requirements.*

G1 A large open-loop gain needs to be attained for frequencies below f_1, i.e., $\underline{\sigma}(P_{s,\text{des}}) \gg 1 \quad \forall \quad f \in [0, f_1]$.

G2 A small open-loop gain needs to be attained for frequencies above f_n, i.e., $\bar{\sigma}(P_{s,\text{des}}) \ll 1 \quad \forall \quad f \in [f_n, f_\infty]$.

The requirements G1–G2 reflect classical closed-loop performance and robustness requirements. To illustrate this statement, consider the target sensitivity function $S_{\text{des}} = (I + P_{s,\text{des}})^{-1}$ and target complementary sensitivity function $T_{\text{des}} = P_{s,\text{dec}}\,(I + P_{s,\text{dec}})^{-1}$. These expressions can be approximated in the relevant frequency range, see [2]:

$$\begin{aligned} \bar{\sigma}(S_{\text{des}}) &\leq \frac{1}{\underline{\sigma}(P_{s,\text{des}})} \ll 1 \;\text{ where } \underline{\sigma}(P_{s,\text{des}}) \gg 1, \\ \bar{\sigma}(T_{\text{des}}) &\leq \bar{\sigma}(P_{s,\text{des}}) \ll 1 \;\text{ where } \bar{\sigma}(P_{s,\text{des}}) \ll 1. \end{aligned} \tag{2}$$

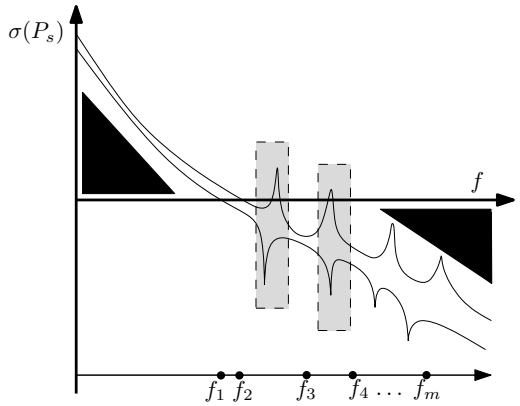

Fig. 2. Loop-shaping singular values P_s for performance and robustness.

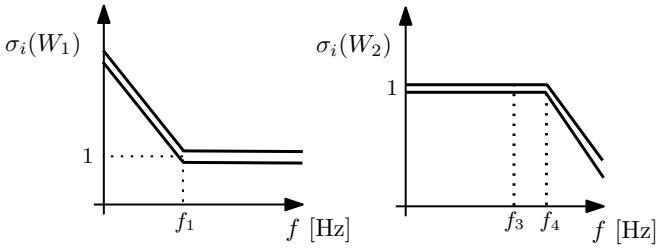

Fig. 3. Classical weighting functions W_1 and W_2.

Expression (2) reveals that $P_{s,\text{des}}$ in Fig. 2 implicitly determines the singular values of S_{des} and T_{des}. Complying with typical requirements, low-frequent disturbances are attenuated if $\bar{\sigma}(S_{\text{des}}) \gg 1$, while $\bar{\sigma}(T_{\text{des}}) \ll 1$ provides robustness with respect to model uncertainty for high-frequencies. This result illustrates the relation between open- and closed-loop weighting functions in Remark 2.

In classical control design, the system is diagonalized in the cross-over region, i.e., $f \in [f_1, f_2]$ determined by $\underline{\sigma}(P_s(f_1)) = 1$ and $\bar{\sigma}(P_s(f_2)) = 1$, by a static decoupling.

Proposition 6. *Let $P \in \mathscr{R}^{n\times n}$. There exist matrices $T_u, T_y \in \mathbb{R}^{n\times n}$ such that*

$$\sigma_i(P_{\text{diag}}) := \sigma_i(T_y P T_u) \approx \left|(T_y P T_u)_{ii}\right|,$$

in $f \in [f_1, f_2]$, where $(T_y P T_u)_{ii}$ is the $(i,i)^{th}$ entry of $T_y P T_u$.

The proof of Prop. 6 follows along similar lines as in [14, Sect. 4.3]. That is, Def. 4 implies that $\tilde{T}_y = U^{-1}$ and $\tilde{T}_u = V^{-H}$, when evaluated in $[f_1, f_2]$. Next, the typically complex matrices $\tilde{T}_y, \tilde{T}_u$ are approximated by $T_u, T_y \in \mathbb{R}^{n\times n}$ by means of the ALIGN algorithm. Proposition 6 implies that P_{diag} can be appended with diagonal W_1 and W_2, such that G1 and G2 are attained. Typically, W_1 defines integral action in $f \in [0, f_1]$, while W_2 specifies roll-off in $f \in [f_4, f_\infty]$. This design is illustrated in Fig. 3. In addition, W_1, W_2 scale P such that the cross-over region of P_s is in $[f_1, f_2]$.

C. Extended requirements for complex multivariable systems

Lightly damped resonance phenomena in $[f_2, f_4]$, as indicated by gray rectangles in Fig. 2, hamper the performance of a system, see, e.g., [15] and [16]. Indeed, in [17, Sect. V] it is illustrated that the dominant components in the servo error stem from such phenomena for an industrial motion system.

The key problem addressed in this paper is the design of W_1, W_2 that accurately reflect performance requirements for lightly damped resonance phenomena in $[f_2, f_4]$, while retaining G1 and G2 in Def. 5. Since the directionality of a system is highly dependent on the dynamical behavior, explicit compensation of the input and output directionality is required for loop-shaping of the gains in $[f_2, f_4]$. To proceed, transformation matrices are determined that provide local compensation of the directionality in distinct frequency ranges. This crucial attribute of the proposed W_1 and W_2 is formulated in the following Sub-Goal.

Sub-Goal 7. *Let $P \in \mathscr{R}^{n\times n}$. Determine matrices $T_{u,j}, T_{y,j} \in \mathbb{R}^{n\times n}$, for $j = 1,\ldots,m$, such that $\forall\ i = 1,\ldots,n$*

$$\sigma_i(T_{u,j} P T_{y,j}) \approx \left|(T_{u,j} P T_{y,j})_{ii}\right| \quad \forall\ f \in [f_j, f_{j+1}].$$

Local compensation of the directionality enables explicit loop-shaping of the gains of P in m distinct frequency ranges. Therefore, the transformation matrices $T_{u,j}, T_{y,j}$ should be absorbed in W_1, W_2 such that P_s satisfies Goal 3. In the next section, $T_{u,j}, T_{y,j}$ are determined that compensate for the directionality of the system in the j^{th} frequency range.

III. LOCAL DIRECTIONALITY COMPENSATION

In this section, a procedure is formulated that is aimed to address Sub-Goal 7. To this purpose, $T_{u,j}, T_{y,j}$ are determined that compensate for the directionality in distinct frequency ranges by exploiting the characteristics of the underlying system. In this paper, the focus is on a class of motion systems.

Definition 8. *[18]*
The dynamical response of a linear motion system $P(s)$ with proportional damping can be written as a sum of N second-order subsystems

$$\begin{aligned} P(s) &= \sum_{i=1}^{n} \frac{c_i^T b_i}{s^2} + \sum_{i=n+1}^{N} \frac{c_i^T b_i}{s^2 + 2\zeta_i \omega_i s + \omega_i^2} \\ &= C P_d(s) B, \end{aligned} \tag{3}$$

with n the number of rigid-body modes, c_i^T the i^{th} column of the output matrix $C \in \mathbb{R}^{n\times N}$, b_i the i^{th} row of the input matrix $B \in \mathbb{R}^{N\times n}$, ζ_i the dimensionless damping constant and ω_i the natural frequency of the i^{th} second-order subsystem.

Typically, a system $P(s)$ is controlled in all n rigid-body degrees of freedom, i.e., the number of inputs and outputs of $P(s)$ is equal to the number of rigid-body modes. Furthermore, note that a rigid-body mode is a second-order subsystem of $P(s)$ with natural frequency $\omega_i = 0$.

For the sake of clarity, transformation matrices $T_{u,j}, T_{y,j}$ are determined for $f \in [0, f_2]$ and $f \in [f_2, f_4]$. Extension of the local directionality compensation method to more frequency ranges is conceptually straightforward. First, transformation matrices $T_{u,1}, T_{y,1}$ are determined that result in compensation of the directionality in $f \in [0, f_2]$.

Proposition 9. *Let $P \in \mathscr{R}^{n\times n}$ comply with Def. 8. Then, there exist $T_{u,1}, T_{y,1} \in \mathbb{R}^{n\times n}$ such that*

$$P_{\text{diag}} := T_{y,1} P T_{u,1},$$

where P_{diag} is diagonal at $s = 0$.

Proof. Let $P_{\text{rb}}(s)$ be defined as

$$P_{\text{rb}}(s) = \sum_{i=1}^{n} \frac{c_i^T b_i}{s^2},$$

i.e., only the n rigid-body modes are considered. Observe that $P_{\text{rb}}(j\omega) \in \mathbb{R}^{n\times n}$. By application of Def. 4 to $P_{\text{rb}}(j\omega) \in \mathbb{R}^{n\times n}$, $\exists U, V \in \mathbb{R}^{n\times n}$ such that $P_{\text{rb,diag}} = T_{y,1} P_{\text{rb}} T_{u,1}$ is diagonal $\forall \omega$, where $T_{y,1} = U^{-1}$ and $T_{u,1} = V^{-T}$. To extend this result to $P(s)$, note that in (3) at $s = 0$, it holds that

$$\sum_{i=1}^{n} \frac{c_i^T b_i}{s^2} \gg \sum_{i=n+1}^{N} \frac{c_i^T b_i}{s^2 + 2\zeta_i \omega_i s + \omega_i^2},$$

which implies that $T_{y,1}, T_{u,1}$ diagonalize (3) at $s = 0$. □

The second-order rigid-body dynamical behavior at $s = 0$ dominates the dynamical response of the system up to frequency f_2. Therefore, for $i = 1,\ldots,n$,

$$\sigma_i(T_{y,1} P T_{u,1}) \approx \left|(T_{y,1} P T_{u,1})_{ii}\right| \quad \forall\ f \in [0, f_2].$$

Second, transformation matrices $T_{u,2}, T_{y,2}$ are determined that provide local compensation of the directionality in $f \in [f_2, f_4]$. Consider the transformed system $P_{\text{flex}}(s)$, representing the resonance phenomena of $P(s)$, given by

$$\begin{aligned} P_{\text{flex}}(s) &:= P(s) - \sum_{i=1}^{n} \frac{c_i^T b_i}{s^2} = \sum_{i=n+1}^{N} \frac{c_i^T b_i}{s^2 + 2\zeta_i \omega_i s + \omega_i^2} \\ &:= C_{\text{flex}} P_{\text{d,flex}}(s) B_{\text{flex}}. \end{aligned}$$

Assumption 10. *The lightly damped resonance phenomena in $[f_2, f_4]$ dominate the dynamical response of $P_{\text{flex}}(s)$ at $s = 0$*

$$\sum_{i=n+1}^{2n} \frac{c_i^T b_i}{\omega_i^2} \gg \sum_{i=2n}^{N} \frac{c_i^T b_i}{\omega_i^2},$$

where

$$P_{\text{flex}}(0) = \sum_{i=n+1}^{2n} \frac{c_i^T b_i}{\omega_i^2} + \sum_{i=2n+1}^{N} \frac{c_i^T b_i}{\omega_i^2}.$$

This assumption is in general non-restrictive for motion systems and is exploited in the following proposition.

Proposition 11. *Given $P_{\text{flex}}(s) \in \mathscr{R}^{n\times n}$, there exist $T_{u,2}, T_{y,2} \in \mathbb{R}^{n\times n}$ such that*

$$P_{\text{flex,diag}} := T_{y,2} P_{\text{flex}}(s) T_{u,2},$$

where $P_{\text{flex,diag}}$ is diagonal at $s = 0$.

The proof of Prop. 11 is similar to the proof provided by Prop. 9. By virtue of Assumption 10, the dynamical response of $P_{\text{flex}}(s)$ is in $f \in [0, f_4]$ dominated by the first n lightly damped resonance phenomena. As a result, for $i = 1,\ldots,n$,

$$\sigma_i(T_{y,2} P_{\text{flex}} T_{u,2}) \approx \left|(T_{y,2} P_{\text{flex}} T_{u,2})_{ii}\right|,$$

in the frequency range $f \in [0, f_4]$.

Although $T_{u,2}, T_{y,2}$ diagonalize $P_{\text{flex}}(s)$ in $[0, f_4]$, $P(s)$ is only diagonalized in the frequency range where the first n

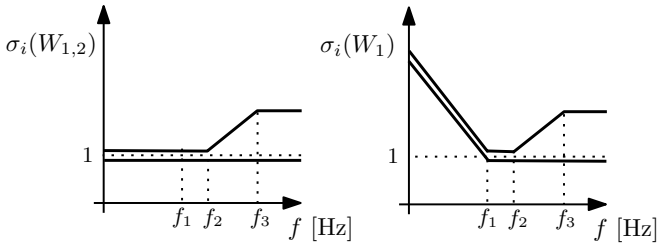

Fig. 4. Weighting $W_{1,2}$ and multivariable weighting function W_1.

resonance phenomena dominate the dynamical response of $P(s)$. In Fig. 2, this corresponds to $[f_2, f_4]$.

Remark 12. *Motion systems according to Def. 8 are a specific class of dyadic systems [19]. It is emphasized that the local directionality compensation proposed in this section is applicable to the general class of dyadic systems.*

The matrices $T_{u,1}$, $T_{y,1}$ and $T_{u,2}$, $T_{y,2}$ constructed in this section should be absorbed in W_1, W_2 to enable explicit loop-shaping of the singular values in respectively $[0, f_2]$ and $[f_2, f_4]$. The proposed weighting function design is discussed in the next section.

IV. FORMULATION OPTIMIZATION CRITERION

A. Multivariable weighting function design

In this section, multivariable weighting functions W_1 and W_2 are proposed for motion systems with pronounced multivariable behavior. These weighting functions reflect i) classical requirements in Def. 5 and ii) compensation of the performance-critical first resonance phenomenon in $[f_2, f_3]$. To satisfy the latter requirement, the directionality of the system should be compensated in $[f_2, f_3]$, as formulated in Sub-Goal 7. Then, the closed-loop performance is improved by specifying damping to the first resonance phenomenon. This leads to the following design procedure for W_1 and W_2, which constitutes the main contribution of this paper.

Procedure 13. *Given $\sigma_i(P_{s,\text{des}})$,*
Classical loop-shaping

Step 1. Determine $T_{y,1}$ and $T_{u,1}$ by applying Prop. 9 to locally compensate for the directionality in $[0, f_2]$.
Step 2. Design $W_{1,1}$ and W_2 that reflect Def. 5, see Fig. 3.

Extended loop-shaping

Step 3. Determine $T_{y,2}$ and $T_{u,2}$ by applying Prop. 11 to locally compensate for the directionality in $[f_2, f_3]$.
Step 4. Construct $W_{1,2}$ for $[f_2, f_3]$ as illustrated in Fig. 4.

Construction W_1 and W_2

Step 5. Integrate $W_{1,1}$ and $W_{1,2}$ in W_1, see Fig. 5.
Step 6. Scale P_s to the target cross-over region $[f_1, f_2]$.

Steps 1-2 have been discussed in Section II-B for classical loop-shaping. Therefore, this section focuses on *Steps 3-4* and *Steps 5-6*, which determine the novel aspect of the proposed weighting function design.

First, consider *Steps 3-4* of Procedure 13. In this part of the procedure, damping is specified to the first lightly damped resonance phenomenon in $[f_2, f_3]$ to improve the closed-loop

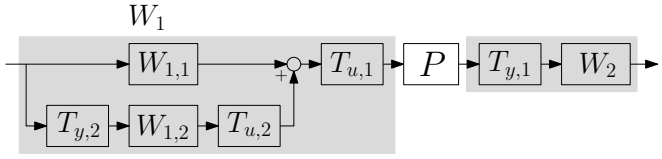

Fig. 5. Multivariable weighting function design.

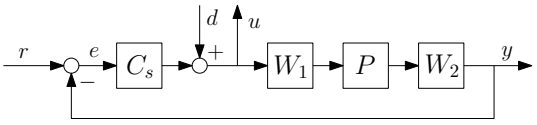

Fig. 6. Weighted feedback configuration.

performance. In [20] it is shown that for a SISO system, the inclusion of derivative action in W_1 for $f \in [f_2, f_3]$ provides damping to this resonance phenomenon. Local compensation of the directionality by means of $T_{y,2}$ and $T_{u,2}$ in *Step 3* enables an extension of this result to multivariable systems.

Second, *Steps 5-6* of Procedure 13 are considered. In *Step 5*, W_1 is constructed from $W_{1,1}$ and $T_{u,2}W_{1,2}T_{y,2}$, as depicted in Fig. 5. The specification of performance requirements in $[0, f_1]$ by $W_{1,1}$ and in $[f_2, f_3]$ by $W_{1,2}$ do not interfere with each other due to the parallel structure of W_1, in conjunction with the high-pass characteristic of $W_{1,2}$ and the low-pass characteristic of $W_{1,1}$, see Fig. 4. Finally, in *Step 6*, P_s is scaled to $[f_1, f_2]$. The resulting P_s achieves Goal 3 for motion systems with pronounced multivariable behavior.

B. Optimal controller synthesis

The multivariable weighting functions constructed in Section IV-A specify the performance and robustness requirements in a scalar optimization criterion. As a final step, the optimal controller C_s^* is determined by minimizing this optimization criterion.

Definition 14. *Let P_s be defined as in Def. 1. Then, the controller C_s^* yields*

$$C_s^* = \arg\min_{C_s} J(P_s, C_s),$$

with $J(P_s, C_s) = ||T(P_s, C_s)||_\infty$ a norm-based criterion.

The considered feedback configuration is depicted in Fig. 6, where $T(P_s, C_s)$ is given by

$$T(P_s, C_s) : \begin{bmatrix} r \\ d \end{bmatrix} \mapsto \begin{bmatrix} y \\ u \end{bmatrix} = \begin{bmatrix} P_s \\ I \end{bmatrix} (I + C_s P_s)^{-1} \begin{bmatrix} C_s & I \end{bmatrix}.$$

The synthesis of the $\mathscr{H}_\infty$-controller C_s^* is extensively treated in [2]. The controller C_s^* is not directly implementable on the real system P. In fact, the controller implemented on P is given by

$$C = W_1 C_s^* W_2.$$

The resulting controller i) guarantees internal stability of the closed-loop system and ii) is $\mathscr{H}_\infty$-optimal with respect to the user-defined performance and robustness requirements.

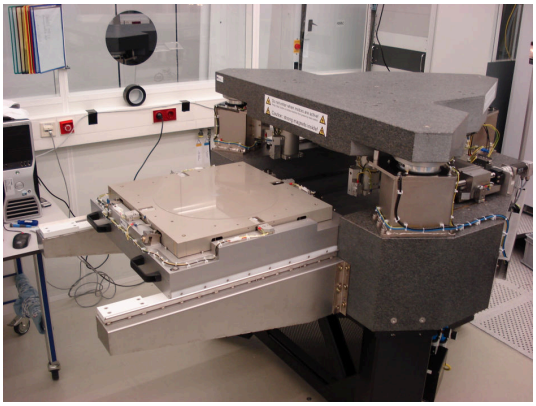

Fig. 7. Experimental setup.

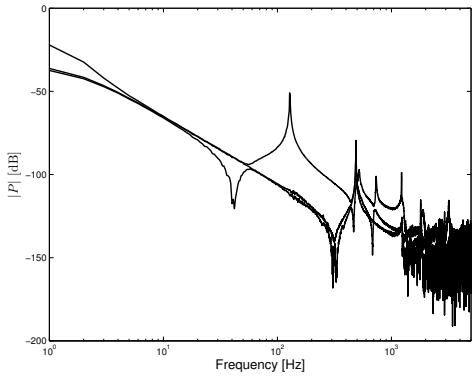

Fig. 8. Singular values of $P(\omega), \omega \in \Omega^{id}$.

V. EXPERIMENTAL RESULTS

A. Experimental setup

In this section, the novel weighting function design proposed in this paper is confronted with a prototype industrial motion system, as depicted in Fig. 7. This prototype is explicitly designed to exhibit pronounced lightly damped resonance phenomena. Such systems are researched in view of the ever-increasing requirements with respect to throughput and accuracy for motion systems in wafer scanners, which are used in semiconductor manufacturing [5]. The experimental setup in Fig. 7 is controlled in all six motion degrees-of-freedom (DOF) (i.e., three rotations and three translations). However, for clarity of exposition, one translational and two rotational DOFs are considered. It is emphasized that the system can be described by Def. 8 in the frequency range of interest. The singular values of the measured frequency response function $P(\omega)$ are depicted in Fig. 8 for $\omega \in \Omega^{id}$, where Ω^{id} is a discrete frequency grid.

B. Weighting function design

In this section, performance and robustness requirements for the experimental setup in Fig. 7 are expressed in weighting functions. First, multivariable weighting functions W_1^{mimo} and W_2^{mimo} are designed according to Proc. 13. Second, classical weighting functions $W_1^{\text{class}}, W_2^{\text{class}}$ are designed based on the guidelines provided in Section II-B. The target crossover region $f = [f_1, f_2]$ is equal to 28 [Hz] in both approaches.

From Fig. 8, it becomes clear that the first resonance phenomenon of $P(\omega)$ appears at 129 [Hz]. Therefore, as depicted in Fig. 9, W_1^{mimo} is designed such that derivative action is specified in $[f_2, f_3] = [28, 250]$ [Hz]. Due to local directionality compensation, only the singular value associated with this resonance phenomenon is weighted in this frequency range. Hence, this approach is not affecting the remaining singular values. Note that the weighting function design is solely based on the experimentally obtained $P(\omega)$.

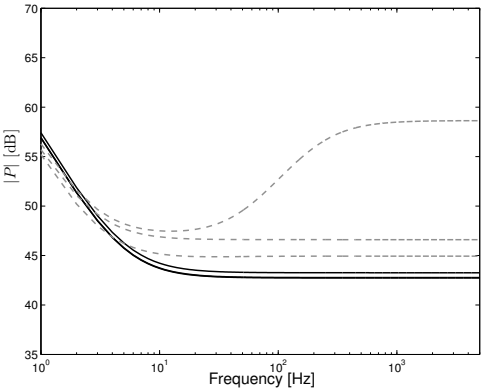

Fig. 9. Singular values of W_1: classical design (black) and multivariable design (dashed grey).

TABLE I

POLES AND DIMENSIONLESS DAMPING COEFFICIENT IN $[f_2, f_3]$.

	$P(s)$	**Classical**	**Multivariable**
Pole	$-3.89 \pm 809i$	$-166 \pm 833i$	$-605 \pm 969i$
ζ	0.00437	0.195	0.529

Finally, the procedure in Sect. IV-B is used to synthesize i) C^{mimo} based on $W_1^{\text{mimo}}, W_2^{\text{mimo}}$ and ii) C^{class} based on $W_1^{\text{class}}, W_2^{\text{class}}$. The parametric model $P(s)$ required for $\mathscr{H}_\infty$-optimization is determined by means of the approach in [17].

C. Analysis

The design of $W_1^{\text{mimo}}, W_2^{\text{mimo}}$ is motivated by the observation in Sect. II-C that lightly damped resonance phenomena hamper the performance of a system. To illustrate the performance enhancement that can be obtained by means of the proposed weighting function design, rejection of disturbances in $[40, 200]$ [Hz] is considered.

The process sensitivity $SP = (I + PC)^{-1}P$ is a suitable measure for disturbance rejection, since SP describes the transfer of input disturbances to the error signal. As depicted in Fig. 10, the singular value of SP associated with the first resonance phenomenon is significantly attenuated in $[40, 200]$ [Hz] as a result of multivariable weighting function design. Note that due to local directionality compensation, $W_1^{\text{mimo}}, W_2^{\text{mimo}}$ only affects this performance-critical singular value of SP, while keeping the remaining singular values unaltered with respect to the classical design.

In $\mathscr{H}_\infty$-optimization, the closed-loop poles in the frequency range $[f_2, f_3]$ are explicitly assigned by the weighting functions and P, see, e.g., [20]. The closed-loop poles for $W_1^{\text{mimo}}, W_2^{\text{mimo}}$ and $W_1^{\text{class}}, W_2^{\text{class}}$ are presented in Table I. The results in this table clearly show that the proposed weighting functions significantly improve the damping of the performance-critical resonance phenomenon at 129 [Hz] when compared to a classical design.

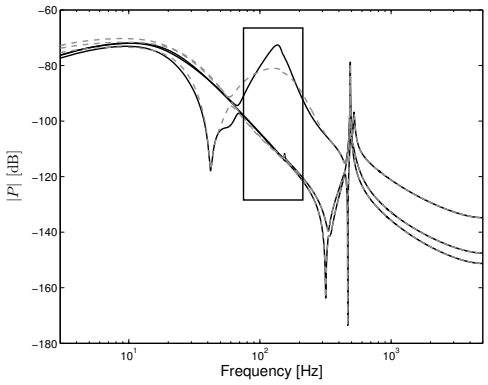

Fig. 10. The singular values of the process sensitivity SP for classical weighting (black) and multivariable weighting functions (dashed gray) show that a significant reduction is obtained in $[40, 200]$ [Hz] as a result of multivariable weighting functions.

TABLE II

STANDARD DEVIATION AND PEAK ERROR SIGNALS.

	σ_1	σ_2	σ_3	p_1	p_2	p_3
C^{class}	0.39	1.57	1.28	1.31	6.12	4.40
C^{mimo}	0.18	0.86	0.60	0.73	3.38	2.30

D. Implementation

The controllers C^{mimo} and C^{class} are implemented on the experimental setup in Fig. 7. An input disturbance with frequency components in $[40, 200]$ [Hz] is applied to the system. The resulting time-domain measurements as depicted in Fig. 11 clearly show that C^{mimo}, based on the proposed multivariable weighting functions in Section IV-A, significantly improves the performance of the system compared to C^{class}, when applied to a prototype high-performance industrial motion system. In addition, Table II confirms that a significant reduction is obtained in the standard deviation and peak value of the error signal in the motion DOFs.

VI. CONCLUSIONS

In this paper, a systematic procedure is developed for the formulation of performance and robustness requirements for a complex multivariable system in $\mathscr{H}_\infty$ control. The weighting functions that define these requirements are inherently multivariable to address the multivariable dynamical behavior of the system, thereby extending pre-existing literature on weighting function design. In particular, characteristics of the underlying system are exploited to enable explicit performance specifications for lightly damped resonance phenomena. A confrontation with a prototype industrial motion system clearly illustrates the performance improvement obtained by means of the proposed multivariable weighting functions, when compared to earlier approaches.

The proposed approach can be directly extended to non-square systems. Furthermore, the results are applicable to i) the class of dyadic systems and ii) sampled-data systems.

In future research, systems are considered that contain a larger number of actuators and sensors than rigid-body DOFs. This introduces additional freedom in the formulation of performance requirements for pronounced lightly damped resonance phenomena in the $\mathscr{H}_\infty$-control framework.

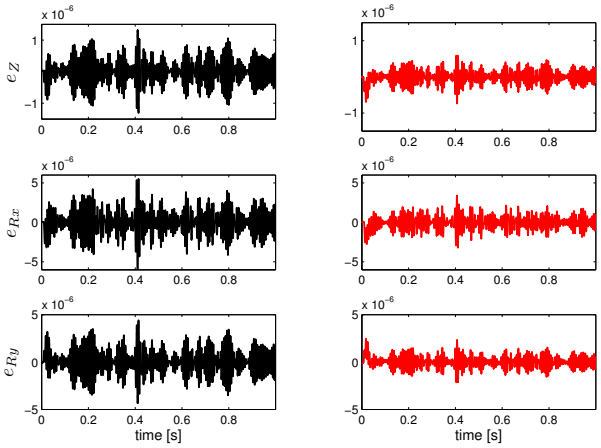

Fig. 11. Measured time domain responses for C^{class} (left) and C^{mimo} (right) show a reduction of approximately 50 [%] in the peak value of the error signal e due to C^{mimo}.

REFERENCES

[1] K. Zhou, J. Doyle, and K. Glover, *Robust and Optimal Control*. Prentice Hall, Upper Saddle River, New Jersey, United States, 1996.

[2] D. McFarlane and K. Glover, *Robust Controller Design Using Normalized Coprime Factor Plant Descriptions*. Springer-Verlag, Berlin, Germany, vol. 138 of Lect. Notes in Control and Inf. Sciences, 1990.

[3] S. Skogestad and I. Postlethwaite, *Multivariable Feedback Control: Analysis and Design*, 2nd ed. John Wiley & Sons, West Sussex, United Kingdom, 2005.

[4] G. Deodhare and M. Vidyasagar, "Every stabilising controller is ℓ_1- and $\mathscr{H}_\infty$ -optimal," *IEEE Transactions on Automatic Control*, vol. 36, no. 9, pp. 1070–1073, 1991.

[5] M. van de Wal, G. van Baars, F. Sperling, and O. Bosgra, "Multivariable $\mathscr{H}_\infty$ / μ feedback control design for high-precision wafer stage motion," *Control Engineering Practice*, vol. 10, pp. 739–755, 2002.

[6] R. Hyde, *$\mathscr{H}_\infty$ aerospace control design - a VSTOL flight application*. Berlin: Springer, Advances in industrial control series, 1995.

[7] M. Steinbuch and M. Norg, "Advanced motion control: An industrial perspective," *European Journal of Control*, vol. 4, pp. 278–293, 1998.

[8] U. Schönhoff and R. Nordman, "A $\mathscr{H}_\infty$-weighting scheme for PID-like motion control," in *Proceedings of the 2002 IEEE International Conference on Control Applications*, 2002, pp. 192–197.

[9] R. Hyde, "The application of robust control to VSTOL aircraft," Ph.D. dissertation, University of Cambridge, 1991.

[10] R. Hyde and K. Glover, "The application of scheduled $\mathscr{H}_\infty$ controllers to a VSTOL aircraft," *IEEE Transactions on Automatic Control*, vol. 38, no. 7, pp. 1021–1039, 1993.

[11] G. Papageorgiou and K. Glover, "A systematic procedure for designing non-diagonal weights to facilitate $\mathscr{H}_\infty$ loop shaping," in *Proc. of the 36th Conference on Decision and Control, San Diego, CA, USA*, 1997.

[12] A. Lanzon, "Weight optimisation in $\mathscr{H}_\infty$ loop-shaping," *Automatica*, vol. 41, no. 7, pp. 1201–1208, 2005.

[13] T. Oomen, M. van de Wal, and O. Bosgra, "Design framework for high-performance optimal sampled-data control with application to a wafer stage," *Int. Journ. of Control*, vol. 80, no. 6, pp. 919–934, 2007.

[14] J. Maciejowski, *Multivariable Feedback Design*. Addison-Weley Publishers Ltd., 1989.

[15] G. Balas and J. Doyle, "Control of lightly damped, flexible modes in the controller crossover region," *Journal of Guidance, Control, and Dynamics*, vol. 17, no. 2, pp. 370–377, 1994.

[16] R. S. Smith, C.-C. Chu, and J. L. Fanson, "The design of $\mathscr{H}_\infty$ controllers for an experimental non-collocated flexible structure problem," *IEEE Transactions on Control Systems Technology*, vol. 2, no. 2, pp. 101–109, 1994.

[17] T. Oomen, R. van Herpen, S. Quist, M. van de Wal, O. Bosgra, and M. Steinbuch, "Connecting system identification and robust control for next-generation motion control of a wafer stage," *IEEE Transactions on Control Systems Technology*, To Appear.

[18] W. Gawronski, *Advanced Structural Dynamics and Active Control of Structures*. Springer, New York, New York, United States, 2004.

[19] D. Owens, *Feedback and multivariable systems*. Peter Peregrinus Ltd., 1978.

[20] L. Cao and Y. Hori, "Mixed sensitivity optimization to avoid pole/zero cancellation," *Automatica*, vol. 33, no. 7, pp. 1379–1385, 1997.